



Published in final edited form as:

*J Immunol.* 2020 May 15; 204(10): 2661–2670. doi:10.4049/jimmunol.1900466.

## IRAK-M regulates monocyte trafficking to the lungs in response to bleomycin challenge.

Brenda F. Reader<sup>\*</sup>, Shruthi Sethurman<sup>\*</sup>, Bryan R. Hay<sup>\*</sup>, Rose Viguna Thomas Becket<sup>\*</sup>, Manjula Karpurapu<sup>\*</sup>, Sangwoon Chung<sup>\*</sup>, Yong Gyu Lee<sup>\*</sup>, John W. Christman<sup>\*</sup>, Megan N. Ballinger<sup>\*</sup>

<sup>\*</sup> Pulmonary, Critical Care and Sleep Medicine, Ohio State University Wexner Medical Center, Davis Heart and Lung Research Institute, Columbus, Ohio 43210

### Abstract

Idiopathic pulmonary fibrosis (IPF) is a deadly disease characterized by excessive extracellular matrix deposition in the lungs resulting in decreased pulmonary function. Although epithelial cells and fibroblasts have long been the focus of IPF research, the role of various subpopulations of macrophages in promoting a fibrotic response is an emerging target. Healthy lungs are composed of two macrophages populations, tissue-resident alveolar macrophages (TR-AMs) and interstitial macrophages, which help to maintain homeostasis. After injury, TR-AMs are depleted and monocytes from the bone marrow (BM) traffic to the lungs along a CCL2/CCR2 axis and differentiate into monocyte-derived AMs (Mo-AMs), which is a cell population implicated in murine models of pulmonary fibrosis. In this study, we sought to determine how IRAK-M, a negative regulator of Toll-like receptor signaling, modulates monocyte trafficking into the lungs in response to bleomycin. Our data indicate that after bleomycin challenge, mice lacking Interleukin-1 receptor-associated kinase (IRAK)-M have decreased monocyte trafficking and reduced Mo-AMs in their lungs. Although IRAK-M expression did not regulate differences in chemokines, cytokines, or adhesion molecules associated with monocyte recruitment, IRAK-M was necessary for CCR2 upregulation following bleomycin challenge. This finding prompted us to develop a competitive BM chimera model, which demonstrated that expression of BM-derived IRAK-M was necessary for monocyte trafficking into the lung and for subsequent enhanced collagen deposition. These data indicate that IRAK-M regulates monocyte trafficking by increasing the expression of CCR2 resulting in enhanced monocyte translocation into the lung, Mo-AM differentiation, and potentiation of the development of pulmonary fibrosis.

### Keywords

monocyte/macrophage; IRAK-M; lung; fibrosis

---

**Corresponding Author: Megan N. Ballinger PhD**, Pulmonary, Critical Care and Sleep Medicine, The Ohio State University Wexner Medical Center, Davis Heart and Lung Research Institute, Columbus, Ohio 43210, Phone: 614-292-6578 Fax: 614-293-4799, Megan.Ballinger@osumc.edu.

**COI statement:** The authors have declared that no conflict of interest exists.

## Introduction

Idiopathic pulmonary fibrosis (IPF) is a chronic, progressive lung disorder characterized by injury, fibroblast hyperplasia, and deposition of extracellular matrix that results in reduced lung elasticity, impaired gas exchange, and decreased pulmonary function. Early IPF is difficult to recognize, and, by the time of diagnosis, well-established IPF portends a poor prognosis (1). Although structural cells in the lungs, like epithelial cells and fibroblasts, are important in the progression of the disease, more recently, it has become apparent that other cell types like macrophages are involved (2). Our work and that of others have focused on the role of macrophages in regulating and possibly propagating the fibrotic response. In healthy lungs, there are two types of resident macrophages: an embryonic yolk sac-derived, self-renewing population present in the alveoli and airways that are referred to as tissue resident alveolar macrophages (TR-AMs) and a population found in the lung interstitium that are referred to as interstitial macrophages (IMs). When mice are challenged with bleomycin, TR-AMs are depleted and peripheral blood monocytes are recruited into the lungs where they differentiate into monocyte-derived alveolar macrophages (Mo-AMs). These recruited, recently differentiated monocytes in the airways previously have been referred to by many different names including: exudate macrophages (3, 4), CD11b<sup>hi</sup> recruited macrophages (5), and monocyte-derived alveolar macrophages (6). In this study, we will call these cells monocyte-derived alveolar macrophage (Mo-AMs) and have identified them with the following flow cytometry gating scheme: CD45<sup>+</sup>Ly6g<sup>-</sup>CD64<sup>+</sup>SiglecF<sup>-</sup>MHCII<sup>hi</sup>CD11b<sup>hi</sup> (7).

An emerging concept is that differentiated Mo-AMs have a distinct functional phenotype and receptor profile expression compared to TR-AMs. This idea aligns well with previous data that have demonstrated reduced collagen deposition in murine models of pulmonary fibrosis when Ly6C<sup>hi</sup> monocyte recruitment is inhibited (8). Furthermore, in these animal models, depletion of Mo-AMs within an injured lung lessens the severity of fibrosis (6, 9). Additionally, in the setting of murine models of lung injury and inflammation, these two macrophage subpopulations have been shown to have different immunometabolic programs and to perform specialized functions (5, 10). Recent studies, using single-cell RNA-Seq, have demonstrated that several macrophage subpopulations exist in the lungs and differentially localize to areas of dense collagen fibers such as those found in fibrotic foci (10, 11). Together, these data suggest that macrophage ontogeny may influence the ability of the cell to respond to the environmental milieu and external stimuli, thus emphasizing the notion that macrophage activation is not a terminal state of differentiation or maturation (12).

Monocytes that have differentiated into macrophages are important in processes like wound healing and repair; however, the stimuli and signal transduction pathways that regulate monocyte trafficking during pulmonary fibrosis have yet to be fully elucidated. It is known that monocytes traffic to the lungs along a positive gradient of CCL2 via the CCR2/CCL2 axis (13). Ly6C<sup>hi</sup> monocytes express increased levels of CCR2, a chemokine receptor that binds to CCL2 and CCL7 and whose expression is restricted to only a few cell populations such as monocytes, fibrocytes, T cells, and a subset of NK cells (13). In response to monocyte chemoattractant signals, Ly6C<sup>hi</sup> monocytes egress from the bone marrow (BM)

into circulation and traffic toward injured or inflamed tissues (14). Additionally, a variety of different transcription factors and signaling pathways have been linked to CCR2 upregulation including: MyD88-dependent TLR signaling (15), FOXM1 (16), NFAT (17), IFN $\gamma$ /STAT1 signaling (18), and PPAR $\gamma$  (19). In addition to mediating monocyte chemoattractant signaling, regulation of these factors and pathways mediates macrophage activation profiles. Work in the field of tissue injury has demonstrated that CCR2<sup>-/-</sup> mice have fewer Ly6C<sup>hi</sup> monocytes at the wound site and slower wound healing times (20). During bleomycin-induced pulmonary fibrosis, mice deficient in CCR2 (CCR2<sup>-/-</sup>) are protected from developing excessive collagen deposition (21). Furthermore, previous studies in patients diagnosed with IPF showed that increased circulating CD14<sup>hi</sup>CD16<sup>hi</sup>CCR2<sup>+</sup> monocytes correlated with worsened disease progression (22). Remarkably, a recent paper has suggested that increased monocyte count in the peripheral blood at the time of diagnosis of IPF was associated with poorer outcomes (23).

In our laboratory using a murine model, we have previously demonstrated that mice deficient in the negative TLR regulator, Interleukin-1 receptor-associated kinase-M (IRAK-M), were protected from excessive collagen deposition following bleomycin challenge (24). Using a BM transplantation model (BMT), we determined that IRAK-M expression in BM-derived cells, rather than structural cells, led to the development of bleomycin-induced pulmonary fibrosis (24). Furthermore, we showed a significant increase in collagen expression during an in vitro co-culture of unchallenged wild-type (WT) fibroblasts with macrophages isolated from WT, but not IRAK-M<sup>-/-</sup>, bleomycin-challenged mice (24). Further characterization of the lung macrophages that were isolated from WT bleomycin-challenged mice identified a profibrotic macrophage phenotype as defined by elevated expression of alternative activation markers (YM1, FIZZ1, and arginase), enhanced STAT6 activation, and increased IL-13 production (24). Here, we tested the hypothesis that IRAK-M expression in BM cells increases expression CCR2 chemokine receptor and modulates the trafficking of immune cells to the lung, thus worsening the pathophysiology of bleomycin-induced pulmonary fibrosis.

## Material and methods

### Animals

A colony of IRAK-M<sup>-/-</sup> (deficient) mice backcrossed onto a C57BL/6 background for more than ten generations was established at The Ohio State University (Columbus, OH). CCR2<sup>-/-</sup> [stock number: 004999], CD45.1 mice [stock number 002014], and C57BL/6J WT [stock number: 000664] were obtained from Jackson Laboratories. For all experiments, mice aged between 6–12 weeks were used and were age- and sex-matched among groups. The animals were housed in specific pathogen-free conditions within The Ohio State University. All animal experiments were performed in compliance with the U.S. Department of Health and Human Services Guide for the Care and Use of Laboratory Animals and were reviewed and approved by the Institutional Animal Care and Use Committee (IACUC) at The Ohio State University.

### Bleomycin-induced pulmonary fibrosis

WT and IRAK-M<sup>-/-</sup> mice were intratracheally (i.t.) administered bleomycin (0.025 U; Sigma). In all figures, day 0 designates unchallenged mice and these mice were compared to mice harvested on days 3, 7, 10, or 14 post-challenge with bleomycin. In a subset of experiments, fibrosis was confirmed by measuring collagen deposition in the lungs by hydroxyproline assay. The hydroxyproline assay was performed using a previous published assay with slight modification (21). Briefly, snap frozen lung tissue is homogenized in PBS with a protease inhibitor (Roche) and incubated with 12N HCl overnight in a 120°C oven. The next day, 5 µl of sample or standard (cis-4-hydroxyl-1 proline, Sigma) was incubated with citrate acetate buffer and chloramine T solution at room temperature for 20 min and then incubated with Ehrlich's solution at 65°C for 20 min. Absorbance was detected on a plate reader at 550 nm, and a standard curve was used to determine the amount of hydroxyproline in the sample.

### Flow cytometry

Cells were isolated by collagenase digestion of murine lungs as previously described (25) or from whole blood collected by heparinized needles and lysed in ACK buffer (Biolegend) according to manufacturer's protocols. Cells were incubated with FcR blocking anti-mouse CD16/32 antibody (BD Biosciences; 2.4G2) followed by specific antibody panels listed in Table 1. Lung cells were then fixed in 2% paraformaldehyde and analyzed on a BD LSR II or LSRFortessa flow cytometer (BD Biosciences) within 2 days and blood cells were not fixed and run immediately after staining. Gating was based on respective unstained cell samples, and data were analyzed with FlowJo software (TreeStar). Specific flow cytometric gating schemes for whole lung digest are presented in Supplemental Figure 1 and for blood samples in Supplemental Figure 4.

### Bronchoalveolar lavage fluid (BALF)

BALF was collected as previously described (26, 27). Briefly, airways were lavaged with PBS and 0.6mM EDTA and total cell counts were analyzed using a Countess Automated Cell Counter (Life Technologies) with Trypan blue exclusion.

### Isolation of macrophages and culture conditions

Macrophages were isolated from the whole lungs of mice by collagenase digestion as previously described (25). Cells were then adherence purified for 1 h in serum-free media at 37°C. Non-adherent cells (such as lymphocytes) were washed away, and adherent cells were incubated overnight at 37°C in complete media (RPMI, 10% FBS, 50 IU/mL penicillin, and 50 µg/mL streptomycin). For BM-derived macrophages (BMDMs), BM cells were isolated from the femurs and tibia of WT or IRAK-M<sup>-/-</sup> mice and differentiated using DMEM supplemented with 10% FBS, 50 IU/mL penicillin, and 50 µg/mL streptomycin. On days 1, 3, and 5, recombinant mouse M-CSF (20 ng/mL) was added, and cells were allowed to differentiate up to 6 days in total.

### **Alveolar epithelial cell (AEC) isolated and culture conditions**

Murine type II AECs were isolated using the method developed by Corti et al. (28) and previously described by others (29).

### **Measurement of cytokines**

CCL2 and GM-CSF were quantitated in BALF, serum and in culture supernatants using ELISAs (R&D Systems) and by following manufacturer's protocols.

### **Quantitative real-time PCR (qPCR)**

RNA was extracted from cells or flash frozen lung tissue homogenates by using a Direct-zol RNA miniPrep Plus Kit (Zymo Research) according to the manufacture's instruction. RNA was quantified using a NanoDrop 1000 Spectrophotometer (ThermoFisher). cDNA synthesis was performed using the RevertAid First Strand cDNA Synthesis Kit (ThermoFisher), and gene expression was measured by qPCR using a QuantStudio 3 Real-Time PCR System using PowerUP SYBR Green Master Mix (Applied Biosystems). A list of forward and reverse primers used for qPCR are provided in Table 2. Data were analyzed by the  $2^{-Ct}$  method with GAPDH expression as the endogenous control.

### **Monocyte and neutrophil mobilization assay**

WT and IRAK-M<sup>-/-</sup> mice were intraperitoneally (i.p.) administered 3 µg of CCL3L1 (R&D Systems) or vehicle as previously described (30). Blood was collected 1 h after treatment using heparinized needles, and specific leukocyte populations were analyzed by flow cytometry as described above. A representative flow dot blot is included in Supplemental Figure 4.

### **Generation of competitive bone marrow (BM) chimeras**

Competitive BM transplantation (BMT) measures the reconstitution of hematopoiesis in lethally-irradiated recipient mice and was used to test the presence and function of hematopoietic stem and progenitor cell populations in the bleomycin-challenged lung. Briefly, recipient CCR2<sup>-/-</sup> mice received 13 Gray of total body irradiation (X-ray source) delivered in two fractions separated by 3 h. BM was harvested from the femurs and tibia of donor WT (CD45.1) and/or IRAK-M<sup>-/-</sup> (CD45.2) mice, and donor cells were transplanted into the lethally-irradiated recipients via tail vein infusion. All experiments that involved mice who underwent BMT were performed 5 weeks post-BMT as previously described (31). Mice were then challenged with bleomycin, and, 10 days after transplantation, flow cytometry was used to distinguish donor from recipient cells. The cells from IRAK-M<sup>-/-</sup> and CCR2<sup>-/-</sup> mice were identified by the presence of CD42.2 allelic variation while cells from WT mice were identified by the presence of the CD42.1 allelic variation. The relative reconstitution of cells in the lung and spleen is shown in Supplemental Figure 6.

### **Statistical analysis**

All data are expressed as mean ± SD and were analyzed using GraphPad Prism 5.0. Comparisons between two experimental groups to determine significance were performed with Student's *t*-test. Comparisons among three or more experimental groups to determine

significance were performed with one-way ANOVA followed by Bonferroni correction to control for multiple comparisons. A value of  $p < 0.05$  was considered significant.

## Results

### Expression of IRAK-M alters macrophage subsets in the lung following bleomycin challenge

In order to assess the role of IRAK-M in the initial acute inflammatory response observed in the bleomycin model, the number of macrophage, monocytes, and neutrophils in the lungs of WT and IRAK-M<sup>-/-</sup> mice were assessed by flow cytometry prior to and at day 3, 7, and 14 days after bleomycin challenge (Figure 1). To measure the specific myeloid-derived cell subpopulations that appear early during the immunological response, various cell populations were distinguished using previously published gating schemes (6) that is illustrated using an untreated WT mouse sample in Supplemental Figure 1A:

Two macrophages populations are present in the lung during homeostasis: alveolar macrophages (AMs) that are cells present in the airspace and interstitial macrophages (IMs) that are present in the tissue. AMs are a heterogeneous cell population that can be further separated into a subpopulation composed of embryonic yolk sac-derived tissue resident AMs (TR-AMs) and a subpopulation derived from circulating monocytes that traffic into the lung (Mo-AMs) after injury or inflammation. A representative figure of the TR-AM and Mo-AM subpopulations in a WT mouse lung after bleomycin challenge is shown in Supplemental Figure 1B. Early after bleomycin challenge, we measured a significant decrease in the total number of TR-AMs and IMs in WT and IRAK-M<sup>-/-</sup> mouse lungs (Figure 1A and 1E). By day 7, the total number of TR-AMs returned to baseline, but there were significantly more IMs present in WT lungs compared to IRAK-M<sup>-/-</sup> lungs. At day 14, the IMs have returned to baseline numbers in both the WT and IRAK-M<sup>-/-</sup> mice. At baseline, relatively few Mo-AMs were present in the WT lungs, but we did observe a significant increase in the number of Mo-AMs in WT, but not IRAK-M<sup>-/-</sup>, lungs at 7 days after bleomycin. However, these numbers returned to baseline by day 14 post-bleomycin challenge (Figure 1B). It is well accepted that monocytes are only present in the bloodstream, and when they enter the tissue, they differentiate into monocyte-derived macrophages (32). In our experiments, the vasculature of the lungs was generously perfused with PBS prior to tissue digestion, yet a large number of monocytes were still present as determined by flow cytometry. The total number of peripheral blood monocytes that remained in the bleomycin-challenged lung after perfusion did not differ between WT and IRAK-M<sup>-/-</sup> mice (Figure 1E); however, significantly higher Ly6c<sup>+</sup> inflammatory monocytes were present in WT mouse lungs at day 3 and continued to day 7 post-bleomycin challenge (Figure 1D). Interestingly, the number of Ly6c<sup>+</sup> inflammatory monocytes was back to baseline by day 14 in both the WT and IRAK-M<sup>-/-</sup> mice (Figure 1C). In all, these data indicate that, in response to bleomycin challenge, IRAK-M modulates monocyte-derived macrophage recruitment to the lung in WT mice. Our data show no difference in the total number of neutrophils in the lungs of WT and IRAK-M<sup>-/-</sup> mice following bleomycin challenge, thus (Figure 1F) indicating that IRAK-M does not impact neutrophil trafficking in the bleomycin model.

### **IRAK-M expression did not regulate differences in expression of monocyte recruiting chemokines and cytokines or in the expression of adhesion molecules**

Previous work has also demonstrated that monocytes are recruited to the lungs in response to several different secreted cellular mediators (13). In our study, we measured the expression of monocyte recruitment chemokines CCL2 and GM-CSF. Although significant increases in the expression of CCL2 (Figure 2A) and GM-CSF (Supplemental Figure 2A) from the alveolar epithelial cells (AECs) were evident at day 3 post-bleomycin challenge, the expression of either chemokine did not differ between WT and IRAK-M<sup>-/-</sup> mice. Furthermore, no significant difference was observed in the amount of GM-CSF in the BAL fluid (BALF) of bleomycin-challenged WT and IRAK-M<sup>-/-</sup> mice (Supplemental Figure 2B). However, by day 7 post-bleomycin challenge, CCL2 was elevated in the BALF of WT, but not IRAK-M<sup>-/-</sup>, mice (Figure 2B). Additionally, no difference in serum levels of CCL2 was observed between the bleomycin-challenged WT and IRAK-M<sup>-/-</sup> mice (Figure 2C). Along with the cell characterization studies shown above, these data indicate that although IRAK-M modestly regulates expression of CCL2, this relationship is not associated with an increase in monocyte-derived lung macrophages in IRAK-M<sup>-/-</sup> mice subjected to the bleomycin challenge.

The translocation of monocytes from circulation into the lung tissue requires the cell to bind to adhesion molecules on the surface of pulmonary microvascular endothelial cells (33). In order to determine whether IRAK-M expression regulates expression of adhesion molecules, ICAM-1, ICAM-2 (LFA-1), and VCAM-1 expression was measured in whole lung tissue following bleomycin challenge. We observed no difference in ICAM-1 expression, a significant decrease in ICAM-2 expression, and a trend towards elevated VCAM-1 expression in both WT and IRAK-M<sup>-/-</sup> mouse lungs after bleomycin challenge (Supplemental Figure 3A-C). Since no differences in adhesion molecule expression were detected between the lungs of WT and IRAK-M<sup>-/-</sup> mice, our data suggest that IRAK-M does not regulate adhesion molecule expression in the lung and that changes in monocyte adhesion to the pulmonary microvascular endothelial cells do not explain differences in the monocyte-derived macrophage population that we observed.

### **Elevated CCR2 expression in WT, but not IRAK-M<sup>-/-</sup>, cells following bleomycin challenge which can cause alterations in macrophage activation markers**

Monocytes are attracted to the lung along a CCL2/CCR2 axis (34). Therefore, we measured the expression of CCR2 in lung cells collected after bleomycin challenge. Beginning at day 3 post-challenge, a significant increase in the mRNA expression of CCR2 in WT, but not IRAK-M<sup>-/-</sup> lung cells was observed (Figure 3A). This increase in CCR2 mRNA expression was associated with an increase in CCR2 expression on lung monocytes as measured by flow cytometry (Figure 3B). In order to verify the role of IRAK-M in regulating monocytes following bleomycin challenge, monocytes were isolated from the blood of WT and IRAK-M<sup>-/-</sup> mice after bleomycin challenge and the total number of monocytes positive for CCR2 as well as the intensity of the CCR2 expression was measured. These data demonstrate that WT, but not IRAK-M<sup>-/-</sup>, mice have elevated monocytes in the blood at day 7 post-bleomycin challenge (Figure 3C), and that these monocytes express higher levels of CCR2 (Figure 3D).

In order to validate the role of CCR2 in regulating monocyte recruitment to the lung in response to injury, WT, IRAK-M<sup>-/-</sup> and CCR2<sup>-/-</sup> mice were challenged with bleomycin and the relative neutrophil, macrophage and monocyte populations present in the lung (Figure 4A) and blood (Figure 4B) were assessed by flow cytometry at day 7. There were significantly lower levels of Mo-AMs in both the IRAK-M<sup>-/-</sup> and CCR2<sup>-/-</sup> mice when compared to WT mice at day 7 post-bleomycin challenge. To order to determine the effect of CCR2 expression in regulating Mo-AMs into the lungs after injury, we measured the relative amounts of neutrophils and monocytes in the blood using the gating scheme shown in Supplemental Figure 4A. Interesting, there were actually increased Ly6c<sup>lo</sup> monocytes in the blood of CCR2<sup>-/-</sup>, demonstrating that the defect of these mice was not in the release of monocytes from the BM, but rather in the trafficking of these cells into the lungs after bleomycin challenge (Figure 4B).

To further investigate interactions between IRAK-K and CCR2 in regulating macrophage function, we isolated BM-derived macrophages (BMDMs) from WT, CCR2<sup>-/-</sup> and IRAK-M<sup>-/-</sup> mice. To assess the role of CCR2 in regulating macrophage activation, BMDMs from WT and CCR2<sup>-/-</sup> mice were stimulated with LPS and IFN $\gamma$  or IL-4 and IL-13 and expression of macrophage activation markers and IRAK-M were measured by qPCR. *In vitro* stimulation with LPS and IFN $\gamma$  resulted in a significant increase in IRAK-M expression in WT, but not CCR2<sup>-/-</sup>, BMDMs (Figure 4C). This is in contrast to other makers of macrophage activation in which IL-4 and IL-13 stimulation resulted in a significant increase in YM1 expression (Figure 4D) and LPS and IFN $\gamma$  stimulation resulted in a significant increase in iNOS expression (Figure 4E). Interestingly, in both cases, expression of macrophage activation markers were significantly reduced in CCR2<sup>-/-</sup> macrophages compared to WT cells. We also measured CCR2 expression on BMDMs from WT and IRAK-M<sup>-/-</sup> mice. These cells were stimulated with LPS overnight and CCR2 expression was measured by flow cytometry. Our data show that there was a significant increase, or shift in the mean fluorescence intensity (MFI), of WT, but not IRAK-M<sup>-/-</sup>, cells after LPS stimulation (Supplemental Figure 5). Together, these data demonstrate that the presence of IRAK-M regulates expression of the monocyte chemokine receptor CCR2 following bleomycin challenge and that this CCR2 expression is associated with the observed differences in the monocyte-derived macrophage populations as well as the altered macrophage activation phenotype observed between bleomycin challenged WT and IRAK-M<sup>-/-</sup> mice.

### Expression of IRAK-M regulates monocyte mobilization following stimulation

In order to determine if IRAK-M regulation of monocyte trafficking was specific to bleomycin challenge, we utilized a previously published model of monocyte and neutrophil mobilization (30). WT and IRAK-M<sup>-/-</sup> mice were treated with a CCL3L1 peptide, a ligand known to induce mobilization of monocytes and neutrophils, and, 1 h later, the relative percentages of neutrophils, Ly6c<sup>hi</sup> inflammatory monocytes, and Ly6c<sup>lo</sup> classical monocytes were assessed in the blood. A representative flow cytometry blot demonstrating the gating strategy to identify the different cellular populations can be found in Supplemental Figure 4. Similar to the findings in our bleomycin model, we demonstrated no difference in the total number of neutrophils in blood of WT and IRAK-M<sup>-/-</sup> mice when challenged with CCL3L1



or vehicle control (Figure 5A). Interestingly, at 1 h post-CCL3L1 treatment, a significant increase in the relative percentages of Ly6c<sup>hi</sup> and Ly6c<sup>lo</sup> monocytes was observed in WT, but not IRAK-M<sup>-/-</sup>, blood (Figure 5B and 5C). Interestingly, the relative percentage of Ly6c<sup>lo</sup> monocytes in the blood of IRAK-M<sup>-/-</sup> mice significantly decreased following CCL3L1 treatment compared to vehicle alone (Figure 5C). These data suggest that regulation of monocyte mobilization and trafficking by IRAK-M is not specific to the bleomycin model and may represent a generalizable impact of IRAK-M.

### Expression of IRAK-M promotes monocyte trafficking to the lung following bleomycin challenge

In order to verify that expression of IRAK-M regulates recruitment of monocytes into the lungs following bleomycin challenge, we established a competitive bone marrow transplant (BMT) model. BM was collected from WT mice (allelic variant identified by CD45.1) and IRAK-M<sup>-/-</sup> mice (allelic variant identified by CD45.2) and transferred either alone or in a competitive combination into lethally-irradiated CCR2<sup>-/-</sup> recipient mice. The recipient mice recovered for 5 weeks before being challenged with bleomycin. At 10 days post-injury, the relative reconstitution rates of the WT or IRAK-M<sup>-/-</sup> cells in the spleen or lung of the recipient CCR2<sup>-/-</sup> mice were measured by flow cytometry using antibodies against CD45.1 or CD45.2. In the mice that received BM from only one donor (either WT or IRAK-M<sup>-/-</sup>), 95% of WT (CD45.1) cells or 98% IRAK-M<sup>-/-</sup> (CD45.2) cells were found in the spleens of CCR2<sup>-/-</sup> recipient mice (Supplemental Figure 6A). As an additional control, we also measured the reconstitution of CCR2<sup>-/-</sup> (CD45.2) into CCR2<sup>-/-</sup> (CD45.2). In the competitive BMT group, which received BM cells from both WT (CD45.1) and IRAK-M<sup>-/-</sup> (CD45.2) mice, approximately 30% WT (CD45.1) cells and 70% IRAK-M<sup>-/-</sup> (CD45.2) cells were found in the spleens of recipient CCR2<sup>-/-</sup> mice (Supplemental Figure 6A). To validate the reconstitution data in the spleen, we also measured relative population in the lung, and found there to be a similar distribution of CD45.1 and CD45.2 cells in the different groups (Supplemental Figure 6B). These data demonstrate the reconstitution of a chimeric BM that comprise cells that are both CD45.1 WT and CD45.2 IRAK-M<sup>-/-</sup> cells.

After bleomycin challenge, lung cells were collected via collagenase digestion of whole lung and monocyte, macrophage and neutrophil populations were assessed by flow cytometry gating as shown in Supplemental Figure 1A. In the competitive BMT group, the ratio of CD45.1 WT and CD45.2 IRAK-M<sup>-/-</sup> neutrophils and TR-AMs were the same as observed in the BMT mice after bleomycin (Figure 6A), which correlates with the reconstitution rate observed in the spleen. Despite the presence of elevated IRAK-M<sup>-/-</sup> CD45.2<sup>+</sup> donor cells overall in the competitive BMT mouse lung, we found that there were significantly more WT CD45.1 IMs, Mo-AMs, classical monocytes, and inflammatory monocytes in the lungs of the competitive chimeric BMT mice after bleomycin challenge (Figure 6A). Together these data indicate that expression of IRAK-M in the BM regulates cellular trafficking in response to bleomycin challenge.

To assess whether IRAK-M expression regulates collagen deposition in the lung following bleomycin challenge, we performed a hydroxyproline assay on the lung tissue of isolated from bleomycin-challenged chimera BMT mice compared to untreated CCR2<sup>-/-</sup> mice. As

previously demonstrated,  $CCR2^{-/-}$  reconstituted with bone marrow from  $CCR2^{-/-}$  were protected from bleomycin-induced pulmonary fibrosis and were not statistically different from  $CCR2^{-/-}$  mice that were untreated.  $CCR2^{-/-}$  recipient mice reconstituted with WT (CD45.1) BM had a marked increase in the collagen deposition in lungs after bleomycin challenge (Figure 6B). Deletion of IRAK-M expression in the BM compartment alone was sufficient to reduce the collagen deposition in the lung after bleomycin challenge as there was no statistical difference between the mice who had a  $IRAK-M^{-/-}$  BMT mice and unchallenged  $CCR2^{-/-}$  control mice (Figure 6B). Furthermore, mice that were reconstituted with both WT and  $IRAK-M^{-/-}$  cells had an intermediate phenotype with significantly higher collagen present in their lungs after bleomycin challenge compared to untreated controls, but no difference was observed when compared to lungs from  $IRAK-M^{-/-}$  BMT mice. All together, these data suggest that IRAK-M modulates extracellular matrix deposition in bleomycin-challenged mice.

## Discussion

Previous work has demonstrated that macrophages derived from recruited monocytes promote pulmonary fibrosis (6, 8, 9); however, the mechanism by which these cells traffic to the lungs following bleomycin challenge had not been defined. In this study, we sought to determine the mechanism by which the presence or absence of IRAK-M enhances monocyte recruitment to the lung. We hypothesized that IRAK-M expression in BM-derived cells increases CCR2 expression and results in increased monocyte trafficking to the lung via the CCL2/CCR2 axis, which promotes bleomycin-induced pulmonary fibrosis.

The main function of the lungs is to facilitate gas exchange and respiration, and, in order to accomplish these lifesaving functions, the lungs have an elegant system of cells that provide structural framework as well as protection against injury and infection. Macrophages are important regulators of lung homeostasis due to their ability to respond to the extracellular milieu by secretion of cytokines and chemokines and phagocytosing of dead cells and cellular debris. Exciting work performed in murine models has utilized both genetic and myeloid cell ablative therapies to interrogate the role of tissue resident and monocyte-derived AMs in the mediating lung injury and repair (6, 8, 9). Although macrophage activation is not a terminal state of differentiation or maturation, these studies have suggested that these newly differentiated macrophages actively participate in lung repair and remodeling. This idea has been further strengthened by recently published work that used single-cell RNA-Seq to examine differences between cells from IPF patients and cells from normal, donor controls (10, 11). These data demonstrated transcriptionally distinct populations of macrophages between diseased and normal tissue. In addition, the studies revealed distinct localization of these newly differentially macrophages to the fibrotic regions of the tissue, which emphasized their ability to exert a profibrotic effect (10). Further understanding of the function of these distinct cellular populations and the mechanism by which these cells are maintained, regulated, and replaced is critical to understanding the pathophysiology of pulmonary fibrosis.

Our lab has demonstrated that  $IRAK-M^{-/-}$  mice are protected from developing bleomycin-induced pulmonary fibrosis (24). Expression of IRAK-M in BM-derived cells resulted in

increased injury and elevated extracellular matrix deposition in the lungs. Macrophages isolated from WT bleomycin-challenged mice had a profibrotic macrophage phenotype as defined by elevated expression of alternative activation markers (YM1, FIZZ1, and arginase), enhanced STAT6 activation, and increased IL-13 production (24). Previous data from other laboratories also indicate that MyD88-dependent signaling pathways regulate CCR2 expression, the chemokine receptor involved in monocyte recruitment (15, 35).

Our current work extends these previous studies and demonstrates a role of IRAK-M expression in regulating monocyte recruitment and macrophage differentiation in the setting of a murine model of bleomycin-induced pulmonary fibrosis. We demonstrated, in response to bleomycin, a significant decrease in the TR-AMs and an increase in CCL2 in the lung by day 7 post-bleomycin challenge, which was independent of IRAK-M expression. Using a previously published flow cytometry gating scheme, we distinguished Mo-AMs from other myeloid cells in the lungs and showed a significant increase in these cells in WT, but not IRAK-M<sup>-/-</sup>, mouse lungs after bleomycin challenge (Figure 1B). In addition, the presence of IRAK-M resulted in upregulated CCR2 expression in the lung and on blood monocytes after bleomycin challenge (Figure 3). Stimulation of CCR2<sup>-/-</sup> BMDMs with LPS and IFN $\gamma$  did not increase expression of IRAK-M in vitro (Figure 4C). Interestingly, treatment of mice with CCL3L1 resulted in elevated number of monocytes in the blood of WT mice when compared to IRAK-M<sup>-/-</sup> mice suggesting the role IRAK-M played in regulating monocyte release from the BM was not dependent on bleomycin challenge (Figure 5). Finally, we established a competitive BMT model by reconstituting CCR2<sup>-/-</sup> mice with a combination of BM from both WT and IRAK-M<sup>-/-</sup> mice. We demonstrated that the presence of IRAK-M resulted in increased numbers of Mo-AMs and increased bleomycin-induced pulmonary fibrosis (Figure 6). Together, our data show that expression of IRAK-M promotes expression of CCR2 resulting in enhanced monocyte release from the BM and trafficking to the lung after injury with bleomycin.

Monocyte-derived macrophages are known to persist in the lung for a long time (6) and are localized to fibrotic regions (10). Previous work in murine models of pulmonary fibrosis have also demonstrated that disruption of the CCR2 signaling pathways protected against the development of pulmonary fibrosis as evidenced by reduced extracellular deposition and diminished collagen expression (21). Monocytes are recruited to areas of injury and inflammation via chemoattractant signals like CCL2, and elevated expression of CCL2 has been found in BALF in both experimental murine models of pulmonary fibrosis and in IPF patients (36). However, a phase 2 clinical trial treating IPF patients with Carlumab, a human monoclonal inhibitory antibody against CCL2, showed no evidence of a treatment benefit compared to those who received placebo (37). It was hypothesized that this inhibitor unexpectedly resulted in a compensatory upregulation of CCL2 and promoted recruitment of CCR2<sup>+</sup> cells to the lung, thus increasing the potential for propagation of the fibrotic response. This possible paradigm holds true for our model as well. Despite the fact that, in our study, Mo-AMs and inflammatory monocytes were elevated in the lungs of WT compared to IRAK-M<sup>-/-</sup> mice (Figure 1 **and** 4), no difference in expression of CCL2 or GM-CSF were detected between these two groups (Figure 2 **and** Supplemental Figure 2).

Although CCR2 is thought to be expressed predominately on monocytes, CCR2 can be found on a variety of other circulating cells such as fibrocytes and T cells as well as structural cells such as endothelial cells, fibroblasts, and alveolar epithelial cells (AECs) (13). In one study, expression of CCR2 on AECs suppressed fibroblast proliferation, a hallmark of pulmonary fibrosis (38). However, it is also possible that the CCL2/CCR2 signaling pathway provides a feedback loop by which macrophages transduce AEC dysfunction (39).

The role of CCR2 in pulmonary fibrosis has been studied using several different murine models of injury and repair. Previous work has demonstrated that CCR2<sup>-/-</sup> mice were protected from bleomycin-induced pulmonary fibrosis (40). Additionally, previous data showed that the increase in circulating CD14<sup>hi</sup>CD16<sup>hi</sup>CCR2<sup>+</sup> monocytes in IPF patients correlated with worsened disease progression (22). In a recent study of the blood of IPF patients, higher numbers of CD14<sup>+</sup> monocyte were correlated with shorter transplant-free survival times and higher mortality, while increased blood T and B cells in were not correlated with poorer outcomes (23). In addition, it has been shown that removal of CCR2<sup>+</sup> cells can protect mice from radiation-induced lung injury (41) and silica-induced fibrosis (42). Furthermore, in a model of familiar interstitial lung disease called Hermansky-Pudlak syndrome, blocking monocyte recruitment into the lungs reduced lung fibrosis (39). On the contrary, in a model of viral infection following BMT, loss of CCR2<sup>+</sup> cells exacerbated the fibrotic response, thus demonstrating that these cells can perform a suppressive role (43). Together, these data suggest that monocyte recruitment, specifically via the CCL2/CCR2 axis, correlated with fibrotic lung disease progression.

Interestingly, a recent article has demonstrated that CCR2 expression is not required for Ly6c<sup>hi</sup> monocyte egress from the BM, but is necessary for inflammatory monocyte recruitment into the brain during viral infections (44). Therefore, understanding the mechanism by which CCR2<sup>+</sup> cells respond to an injury and their role once they traffic to the lung are important for the development of novel therapeutics to inhibit and possibly reverse fibrosis. For example, the use of cenicriviroc (CVC), an oral dual chemokine receptor CCR2/CCR5 antagonist, reduced accumulation of Ly6c<sup>+</sup> monocyte-derived macrophages in an experimental model of liver fibrosis (45). Overall, in regards to treatment of IPF, therapeutic approaches to target CCR2-mediated cellular recruitment into the lungs could allow for disruption of cellular interactions and inhibition of signaling pathways that perpetuate the fibrotic signal.

One issue previously raised was that monocytes exist in the bloodstream, but once they translocate into an organ, they differentiate into macrophages. Therefore, in order to eliminate possible blood monocyte contamination of the lung, several groups have proposed to use an injection of CD45-labeled antibody intravenously immediately before euthanasia to be able to distinguish monocytes in the blood compared to those present in the tissue. Initial studies using this protocol did not yield any difference in the number of monocytes calculated in our models after bleomycin challenge (data not shown). One possible explanation was that our previous publication demonstrated that bleomycin challenge results increased alveolar permeability as measured by the elevated albumin in the BALF (24). One limitation to our current study is that previous work has also demonstrated that CCL2

stimulates the surface expression of CX3CR1, which is another chemokine expressed on monocytes (46). CX3CR1 may also play a role in trafficking cells to the site of injury during pulmonary fibrosis, but was not examined in these studies. Additional ongoing work in our lab will investigate the expression of this chemokine receptor in our model.

In summary, our data demonstrate that genetic ablation of IRAK-M in BM-derived cells results in decreased monocyte trafficking to the lung and attenuates the accumulation of collagen deposition during bleomycin-induced pulmonary fibrosis. Additionally, our data suggest that the significant decrease in the expression of CCR2 in IRAK-M<sup>-/-</sup> mice may have contributed to the protection from developing bleomycin-induced pulmonary fibrosis. We interpret these data to indicate a pathological role for IRAK-M in regulating monocyte trafficking by upregulating the expression of CCR2 on peripheral blood monocytes, thus promoting monocyte-derived macrophage recruitment and the development of pulmonary fibrosis. Overall, these data suggest that CCR2 may be a viable point of therapeutic intervention for diseases like IPF.

## Supplementary Material

Refer to Web version on PubMed Central for supplementary material.

## Acknowledgements

We would like to thank Dr. Richard Flavell at Yale University for the original IRAK-M<sup>-/-</sup> mice. In addition, we would like to thank the analytical flow cytometry core (P30CA016058) for their technical assistance and the Davis Heart and Lung Research Institute at The Ohio State University.

### Funding sources

This work was supported by grants from the National Institute of Health (R01HL141217 and R01HL137224) by M.N.B and J.W.C, American Heart Association/SDG grant (M.N.B and M.K.), and the American Thoracic Society Research Foundation (M.N.B.).

## Abbreviation list

<b>AEC</b>	alveolar epithelial cells
<b>AMs</b>	alveolar macrophages
<b>BM</b>	bone marrow
<b>BMT</b>	bone marrow transplantation
<b>BMDMs</b>	bone marrow-derived macrophages
<b>IMs</b>	interstitial macrophages
<b>IPF</b>	idiopathic pulmonary fibrosis
<b>IRAK-M</b>	interleukin-1 receptor-associated kinase-M
<b>Mo-AMs</b>	monocyte-derived alveolar macrophages
<b>TR-AMs</b>	tissue resident alveolar macrophages

WT wild-type

## References Cited

1. Raghu G, Chen SY, Hou Q, Yeh WS, and Collard HR 2016 Incidence and prevalence of idiopathic pulmonary fibrosis in US adults 18–64 years old. *Eur Respir J*.
2. Desai O, Winkler J, Minasyan M, and Herzog EL 2018 The Role of Immune and Inflammatory Cells in Idiopathic Pulmonary Fibrosis. *Front Med (Lausanne)* 5: 43. [PubMed: 29616220]
3. Osterholzer JJ, Olszewski MA, Murdock BJ, Chen GH, Erb-Downward JR, Subbotina N, Browning K, Lin Y, Morey RE, Dayrit JK, Horowitz JC, Simon RH, and Sisson TH 2013 Implicating exudate macrophages and Ly-6C(high) monocytes in CCR2-dependent lung fibrosis following gene-targeted alveolar injury. *J Immunol* 190: 3447–3457. [PubMed: 23467934]
4. Tighe RM, Liang J, Liu N, Jung Y, Jiang D, Gunn MD, and Noble PW 2011 Recruited exudative macrophages selectively produce CXCL10 after noninfectious lung injury. *Am J Respir Cell Mol Biol* 45: 781–788. [PubMed: 21330464]
5. Mould KJ, Barthel L, Mohning MP, Thomas SM, McCubbrey AL, Danhorn T, Leach SM, Fingerlin TE, O'Connor BP, Reisz JA, D'Alessandro A, Bratton DL, Jakubzick CV, and Janssen WJ 2017 Cell Origin Dictates Programming of Resident versus Recruited Macrophages during Acute Lung Injury. *Am J Respir Cell Mol Biol* 57: 294–306. [PubMed: 28421818]
6. Misharin AV, Morales-Nebreda L, Reyfman PA, Cuda CM, Walter JM, McQuattie-Pimentel AC, Chen CI, Anekalla KR, Joshi N, Williams KJN, Abdala-Valencia H, Yacoub TJ, Chi M, Chiu S, Gonzalez-Gonzalez FJ, Gates K, Lam AP, Nicholson TT, Homan PJ, Soberanes S, Dominguez S, Morgan VK, Saber R, Shaffer A, Hinchcliff M, Marshall SA, Bharat A, Berdnikovs S, Borhade SM, Bartom ET, Morimoto RI, Balch WE, Sznajder JI, Chandel NS, Mutlu GM, Jain M, Gottardi CJ, Singer BD, Ridge KM, Bagheri N, Shilatifard A, Budinger GRS, and Perlman H 2017 Monocyte-derived alveolar macrophages drive lung fibrosis and persist in the lung over the life span. *J Exp Med* 214: 2387–2404. [PubMed: 28694385]
7. Ballinger MN, and Christman JW 2016 Pulmonary Macrophages: Overlooked and Underappreciated. *Am J Respir Cell Mol Biol* 54: 1–2. [PubMed: 26720905]
8. Gibbons MA, MacKinnon AC, Ramachandran P, Dhaliwal K, Duffin R, Phythian-Adams AT, van Rooijen N, Haslett C, Howie SE, Simpson AJ, Hirani N, Gauldie J, Iredale JP, Sethi T, and Forbes SJ 2011 Ly6Chi monocytes direct alternatively activated profibrotic macrophage regulation of lung fibrosis. *Am J Respir Crit Care Med* 184: 569–581. [PubMed: 21680953]
9. McCubbrey AL, Barthel L, Mohning MP, Redente EF, Mould KJ, Thomas SM, Leach SM, Danhorn T, Gibbings SL, Jakubzick CV, Henson PM, and Janssen WJ 2018 Deletion of c-FLIP from CD11b(hi) Macrophages Prevents Development of Bleomycin-induced Lung Fibrosis. *Am J Respir Cell Mol Biol* 58: 66–78. [PubMed: 28850249]
10. Aran D, Looney AP, Liu L, Wu E, Fong V, Hsu A, Chak S, Naikawadi RP, Wolters PJ, Abate AR, Butte AJ, and Bhattacharya M 2019 Reference-based analysis of lung single-cell sequencing reveals a transitional profibrotic macrophage. *Nat Immunol* 20: 163–172. [PubMed: 30643263]
11. Reyfman PA, Walter JM, Joshi N, Anekalla KR, McQuattie-Pimentel AC, Chiu S, Fernandez R, Akbarpour M, Chen CI, Ren Z, Verma R, Abdala-Valencia H, Nam K, Chi M, Han S, Gonzalez-Gonzalez FJ, Soberanes S, Watanabe S, Williams KJN, Flozak AS, Nicholson TT, Morgan VK, Winter DR, Hinchcliff M, Hrusch CL, Guzy RD, Bonham CA, Sperling AI, Bag R, Hamanaka RB, Mutlu GM, Yeldandi AV, Marshall SA, Shilatifard A, Amaral LAN, Perlman H, Sznajder JI, Argento AC, Gillespie CT, Dematte J, Jain M, Singer BD, Ridge KM, Lam AP, Bharat A, Borhade SM, Gottardi CJ, Budinger GRS, and Misharin AV 2018 Single-Cell Transcriptomic Analysis of Human Lung Provides Insights into the Pathobiology of Pulmonary Fibrosis. *Am J Respir Crit Care Med*.
12. Morales-Nebreda L, Misharin AV, Perlman H, and Budinger GR 2015 The heterogeneity of lung macrophages in the susceptibility to disease. *Eur Respir Rev* 24: 505–509. [PubMed: 26324812]
13. Shi C, and Pamer EG 2011 Monocyte recruitment during infection and inflammation. *Nat Rev Immunol* 11: 762–774. [PubMed: 21984070]

14. Fujimura N, Xu B, Dalman J, Deng H, Aoyama K, and Dalman RL 2015 CCR2 inhibition sequesters multiple subsets of leukocytes in the bone marrow. *Sci Rep* 5: 11664. [PubMed: 26206182]
15. Pietras EM, Miller LS, Johnson CT, O'Connell RM, Dempsey PW, and Cheng G 2011 A MyD88-dependent IFN $\gamma$ -CCR2 signaling circuit is required for mobilization of monocytes and host defense against systemic bacterial challenge. *Cell Res* 21: 1068–1079. [PubMed: 21467996]
16. Ren X, Zhang Y, Snyder J, Cross ER, Shah TA, Kalin TV, and Kalinichenko VV 2010 Forkhead box M1 transcription factor is required for macrophage recruitment during liver repair. *Mol Cell Biol* 30: 5381–5393. [PubMed: 20837707]
17. Jung H, and Miller RJ 2008 Activation of the nuclear factor of activated T-cells (NFAT) mediates upregulation of CCR2 chemokine receptors in dorsal root ganglion (DRG) neurons: a possible mechanism for activity-dependent transcription in DRG neurons in association with neuropathic pain. *Mol Cell Neurosci* 37: 170–177. [PubMed: 17949992]
18. Hu X, Park-Min KH, Ho HH, and Ivashkiv LB 2005 IFN- $\gamma$ -primed macrophages exhibit increased CCR2-dependent migration and altered IFN- $\gamma$  responses mediated by Stat1. *J Immunol* 175: 3637–3647. [PubMed: 16148108]
19. Chen Y, Green SR, Ho J, Li A, Almazan F, and Quehenberger O 2005 The mouse CCR2 gene is regulated by two promoters that are responsive to plasma cholesterol and peroxisome proliferator-activated receptor gamma ligands. *Biochem Biophys Res Commun* 332: 188–193. [PubMed: 15896316]
20. Boniakowski AE, Kimball AS, Joshi A, Schaller M, Davis FM, denDekker A, Obi AT, Moore BB, Kunkel SL, and Gallagher KA 2018 Murine macrophage chemokine receptor CCR2 plays a crucial role in macrophage recruitment and regulated inflammation in wound healing. *Eur J Immunol* 48: 1445–1455. [PubMed: 29879295]
21. Moore BB, Paine R 3rd, Christensen PJ, Moore TA, Sitterding S, Ngan R, Wilke CA, Kuziel WA, and Toews GB 2001 Protection from pulmonary fibrosis in the absence of CCR2 signaling. *J Immunol* 167: 4368–4377. [PubMed: 11591761]
22. Moore BB, Fry C, Zhou Y, Murray S, Han MK, Martinez FJ, Flaherty KR, and The CI 2014 Inflammatory leukocyte phenotypes correlate with disease progression in idiopathic pulmonary fibrosis. *Front Med* 1.
23. Scott MKD, Quinn K, Li Q, Carroll R, Warsinske H, Vallania F, Chen S, Carns MA, Aren K, Sun J, Koloms K, Lee J, Baral J, Kropski J, Zhao H, Herzog E, Martinez FJ, Moore BB, Hinchcliff M, Denny J, Kaminski N, Herazo-Maya JD, Shah NH, and Khatri P 2019 Increased monocyte count as a cellular biomarker for poor outcomes in fibrotic diseases: a retrospective, multicentre cohort study. *Lancet Respir Med*.
24. Ballinger MN, Newstead MW, Zeng X, Bhan U, Mo XM, Kunkel SL, Moore BB, Flavell R, Christman JW, and Standiford TJ 2015 IRAK-M promotes alternative macrophage activation and fibroproliferation in bleomycin-induced lung injury. *J Immunol* 194: 1894–1904. [PubMed: 25595781]
25. Deng JC, Cheng G, Newstead MW, Zeng X, Kobayashi K, Flavell RA, and Standiford TJ 2006 Sepsis-induced suppression of lung innate immunity is mediated by IRAK-M. *J Clin Invest* 116: 2532–2542. [PubMed: 16917541]
26. Lee YG, Jeong JJ, Nyenhuis S, Berdyshev E, Chung S, Ranjan R, Karpurapu M, Deng J, Qian F, Kelly EA, Jarjour NN, Ackerman SJ, Natarajan V, Christman JW, and Park GY 2014 Recruited Alveolar Macrophages, in Response to Airway Epithelial-derived MCP-1/CCL2, Regulate Airway Inflammation and Remodeling in Allergic Asthma. *Am J Respir Cell Mol Biol*.
27. Qian F, Deng J, Lee YG, Zhu J, Karpurapu M, Chung S, Zheng JN, Xiao L, Park GY, and Christman JW 2015 The transcription factor PU.1 promotes alternative macrophage polarization and asthmatic airway inflammation. *Journal of molecular cell biology* 7: 557–567. [PubMed: 26101328]
28. Corti M, Brody AR, and Harrison JH 1996 Isolation and primary culture of murine alveolar type II cells. *Am J Respir Cell Mol Biol* 14: 309–315. [PubMed: 8600933]
29. Ballinger MN, Newstead MW, Zeng X, Bhan U, Horowitz JC, Moore BB, Pinsky DJ, Flavell RA, and Standiford TJ 2012 TLR signaling prevents hyperoxia-induced lung injury by protecting the alveolar epithelium from oxidant-mediated death. *J Immunol* 189: 356–364. [PubMed: 22661086]

30. Massara M, Bonavita O, Savino B, Caronni N, Mollica Poeta V, Sironi M, Setten E, Recordati C, Crisafulli L, Ficara F, Mantovani A, Locati M, and Bonecchi R 2018 ACKR2 in hematopoietic precursors as a checkpoint of neutrophil release and anti-metastatic activity. *Nat Commun* 9: 676. [PubMed: 29445158]
31. Hubbard LL, Ballinger MN, Wilke CA, and Moore BB 2008 Comparison of conditioning regimens for alveolar macrophage reconstitution and innate immune function post bone marrow transplant. *Experimental lung research* 34: 263–275. [PubMed: 18465404]
32. Swirski FK, Nahrendorf M, Etzrodt M, Wildgruber M, Cortez-Retamozo V, Panizzi P, Figueiredo JL, Kohler RH, Chudnovskiy A, Waterman P, Aikawa E, Mempel TR, Libby P, Weissleder R, and Pittet MJ 2009 Identification of splenic reservoir monocytes and their deployment to inflammatory sites. *Science* 325: 612–616. [PubMed: 19644120]
33. Dragoni S, Hudson N, Kenny BA, Burgoyne T, McKenzie JA, Gill Y, Blaber R, Futter CE, Adamson P, Greenwood J, and Turowski P 2017 Endothelial MAPKs Direct ICAM-1 Signaling to Divergent Inflammatory Functions. *J Immunol* 198: 4074–4085. [PubMed: 28373581]
34. Maus UA, Waelsch K, Kuziel WA, Delbeck T, Mack M, Blackwell TS, Christman JW, Schlondorff D, Seeger W, and Lohmeyer J 2003 Monocytes are potent facilitators of alveolar neutrophil emigration during lung inflammation: role of the CCL2-CCR2 axis. *J Immunol* 170: 3273–3278. [PubMed: 12626586]
35. Serbina NV, Hohl TM, Cherny M, and Pamer EG 2009 Selective expansion of the monocytic lineage directed by bacterial infection. *J Immunol* 183: 1900–1910. [PubMed: 19596996]
36. Moore BB 2014 Following the path of CCL2 from prostaglandins to periostin in lung fibrosis. *Am J Respir Cell Mol Biol* 50: 848–852. [PubMed: 24605795]
37. Raghu G, Martinez FJ, Brown KK, Costabel U, Cottin V, Wells AU, Lancaster L, Gibson KF, Haddad T, Agarwal P, Mack M, Dasgupta B, Nnane IP, Flavin SK, and Barnathan ES 2015 CC-chemokine ligand 2 inhibition in idiopathic pulmonary fibrosis: a phase 2 trial of carlumab. *Eur Respir J* 46: 1740–1750. [PubMed: 26493793]
38. Moore BB, Peters-Golden M, Christensen PJ, Lama V, Kuziel WA, Paine R 3rd, and Toews GB 2003 Alveolar epithelial cell inhibition of fibroblast proliferation is regulated by MCP-1/CCR2 and mediated by PGE2. *Am J Physiol Lung Cell Mol Physiol* 284: L342–349. [PubMed: 12388376]
39. Young LR, Gulleman PM, Short CW, Tanjore H, Sherrill T, Qi A, McBride AP, Zaynagetdinov R, Benjamin JT, Lawson WE, Novitskiy SV, and Blackwell TS 2016 Epithelial-macrophage interactions determine pulmonary fibrosis susceptibility in Hermansky-Pudlak syndrome. *JCI Insight* 1: e88947. [PubMed: 27777976]
40. Okuma T, Terasaki Y, Kaikita K, Kobayashi H, Kuziel WA, Kawasuji M, and Takeya M 2004 C-C chemokine receptor 2 (CCR2) deficiency improves bleomycin-induced pulmonary fibrosis by attenuation of both macrophage infiltration and production of macrophage-derived matrix metalloproteinases. *J Pathol* 204: 594–604. [PubMed: 15538737]
41. Groves AM, Johnston CJ, Williams JP, and Finkelstein JN 2018 Role of Infiltrating Monocytes in the Development of Radiation-Induced Pulmonary Fibrosis. *Radiat Res* 189: 300–311. [PubMed: 29332538]
42. Lebrun A, Lo Re S, Chantry M, Izquierdo Carrera X, Uwambayinema F, Ricci D, Devosse R, Ibouaaden S, Brombin L, Palmari-Pallag M, Yakoub Y, Pasparakis M, Lison D, and Huaux F 2017 CCR2(+) monocytic myeloid-derived suppressor cells (M-MDSCs) inhibit collagen degradation and promote lung fibrosis by producing transforming growth factor-beta1. *J Pathol* 243: 320–330. [PubMed: 28799208]
43. Gurczynski SJ, Procaro MC, O'Dwyer DN, Wilke CA, and Moore BB 2016 Loss of CCR2 signaling alters leukocyte recruitment and exacerbates gamma-herpesvirus-induced pneumonitis and fibrosis following bone marrow transplantation. *Am J Physiol Lung Cell Mol Physiol* 311: L611–627. [PubMed: 27448666]
44. Winkler CW, Woods TA, Robertson SJ, McNally KL, Carmody AB, Best SM, and Peterson KE 2018 Cutting Edge: CCR2 Is Not Required for Ly6C(hi) Monocyte Egress from the Bone Marrow but Is Necessary for Migration within the Brain in La Crosse Virus Encephalitis. *J Immunol* 200: 471–476. [PubMed: 29246952]



45. Krenkel O, Puengel T, Govaere O, Abdallah AT, Mossanen JC, Kohlhepp M, Liepelt A, Lefebvre E, Luedde T, Hellerbrand C, Weiskirchen R, Longerich T, Costa IG, Anstee QM, Trautwein C, and Tacke F 2018 Therapeutic inhibition of inflammatory monocyte recruitment reduces steatohepatitis and liver fibrosis. *Hepatology* 67: 1270–1283. [PubMed: 28940700]
46. Green SR, Han KH, Chen Y, Almazan F, Charo IF, Miller YI, and Quehenberger O 2006 The CC chemokine MCP-1 stimulates surface expression of CX3CR1 and enhances the adhesion of monocytes to fractalkine/CX3CL1 via p38 MAPK. *J Immunol* 176: 7412–7420. [PubMed: 16751386]

**Key points**

TLR signaling pathway regulates expression of monocyte chemoattractant, CCR2.  
IRAK-M is important regulator of monocyte trafficking to the lung in fibrosis.

Author Manuscript

Author Manuscript

Author Manuscript

Author Manuscript

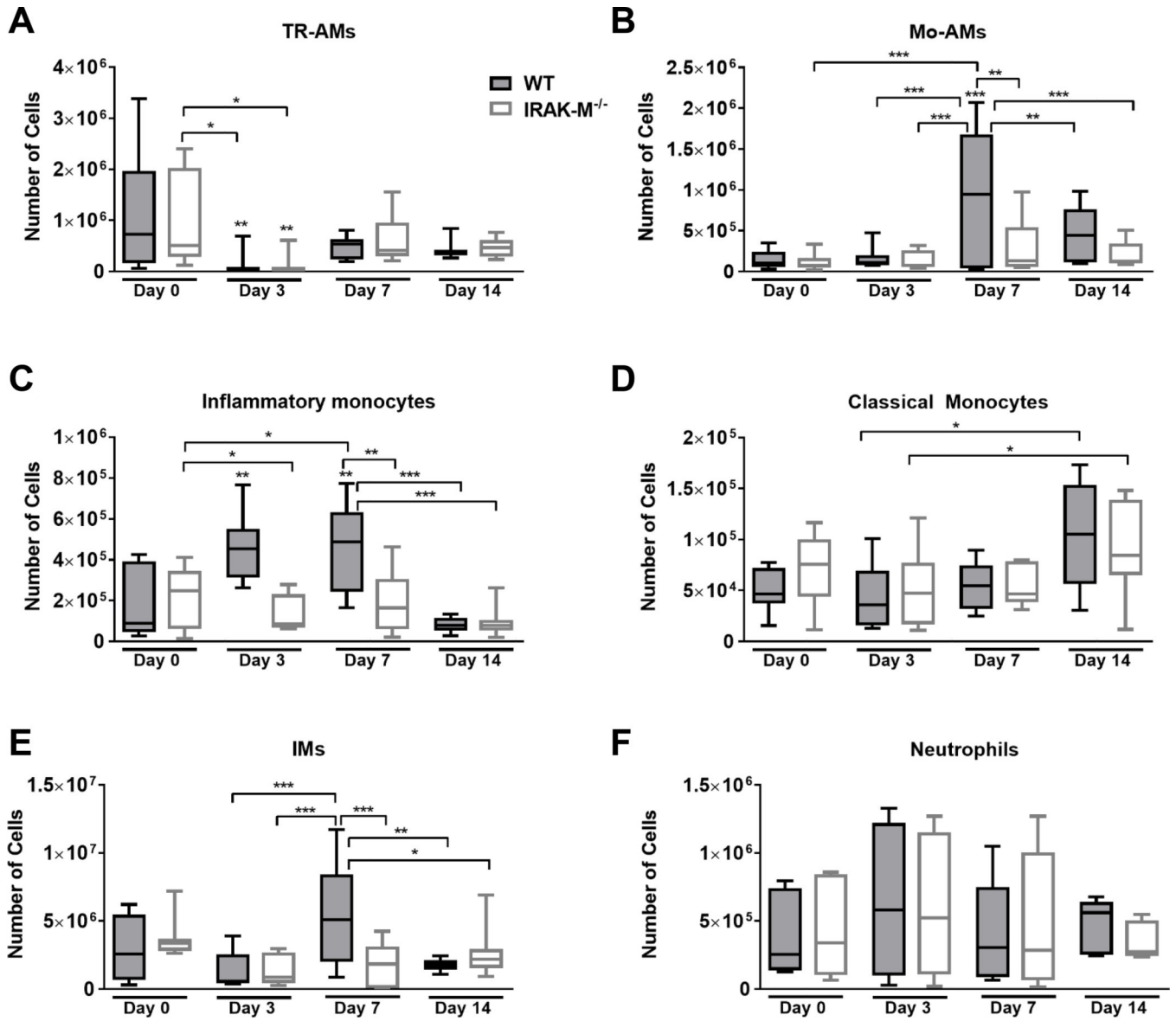


**Figure 1: Expression of IRAK-M alters monocyte trafficking and macrophage subpopulations in the lung following bleomycin challenge.**

WT and IRAK-M<sup>-/-</sup> mice were challenged with bleomycin (i.t.) and whole lung tissue was digested as described in the Material and Methods section. Expression of various myeloid cell populations were determine by flow cytometry (gating scheme shown in Supplemental Figure 1A). Expression of (A) tissue-resident alveolar macrophages (TR-AMs) as measured by CD45<sup>+</sup>Ly6g<sup>-</sup>CD11c<sup>+</sup>CD64<sup>+</sup>SigF<sup>hi</sup>, (B) monocyte-derived alveolar macrophages (Mo-AMs) as measured by CD45<sup>+</sup>Ly6g<sup>-</sup>CD11c<sup>+</sup>CD64<sup>+</sup>SigF<sup>lo</sup>, (C) interstitial macrophages (IMs) as measured by CD45<sup>+</sup>Ly6g<sup>-</sup>CD64<sup>+</sup>SigF<sup>-</sup>MHCII<sup>+</sup>CD11b<sup>+</sup>, (D) inflammatory monocytes as measured by CD45<sup>+</sup>Ly6g<sup>-</sup>MHCII<sup>-</sup>CD64<sup>+</sup>CD11b<sup>+</sup>CD11c<sup>-</sup>Ly6c<sup>+</sup>, (E) classical monocytes as measured by CD45<sup>+</sup>Ly6g<sup>-</sup>MHCII<sup>-</sup>CD64<sup>+</sup>CD11b<sup>+</sup>CD11c<sup>-</sup>Ly6c<sup>-</sup>, and (F) neutrophils as measured by CD45<sup>+</sup>Ly6g<sup>+</sup> cells were determined at day 0, 3, 7, and 14 following bleomycin challenge. Data represent the analysis of n=8 mice/group. Statistical

significance was determined by one-way ANOVA with Bonferroni correction. The asterisks (\*) represent statistical differences \* $p < 0.05$ , \*\* $p < 0.01$ , \*\*\* $p < 0.001$  compared to WT controls or as indicated with significance lines between groups.

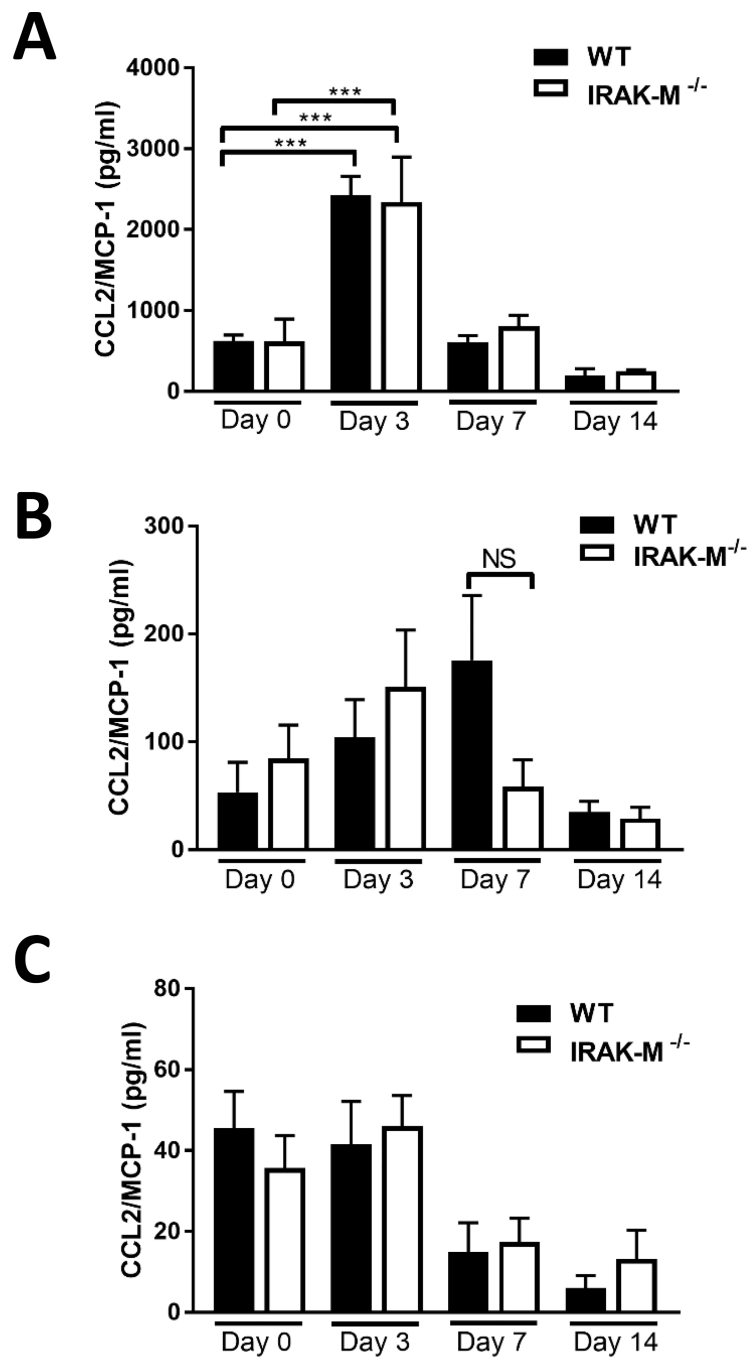


**Figure 2: No differences in CCL2 production between WT and IRAK-M<sup>-/-</sup> mice after bleomycin challenge**

WT and IRAK-M<sup>-/-</sup> mice were challenged with bleomycin (i.t.). Production of MCP-1/CCL2 was assessed by specific ELISA in (A) isolated alveolar epithelial cells (AEC) and (n=5 samples/group), (B) BALF (n=4 samples/group), and (C) serum (n=3 samples/group) at the time points indicated. Data are representative of the analysis of the ELISA assay which was repeated 2 times. Statistical significance was determined by one-way ANOVA with Bonferroni correction. The asterisks (\*) represent statistical differences \*\*\*p<0.001.

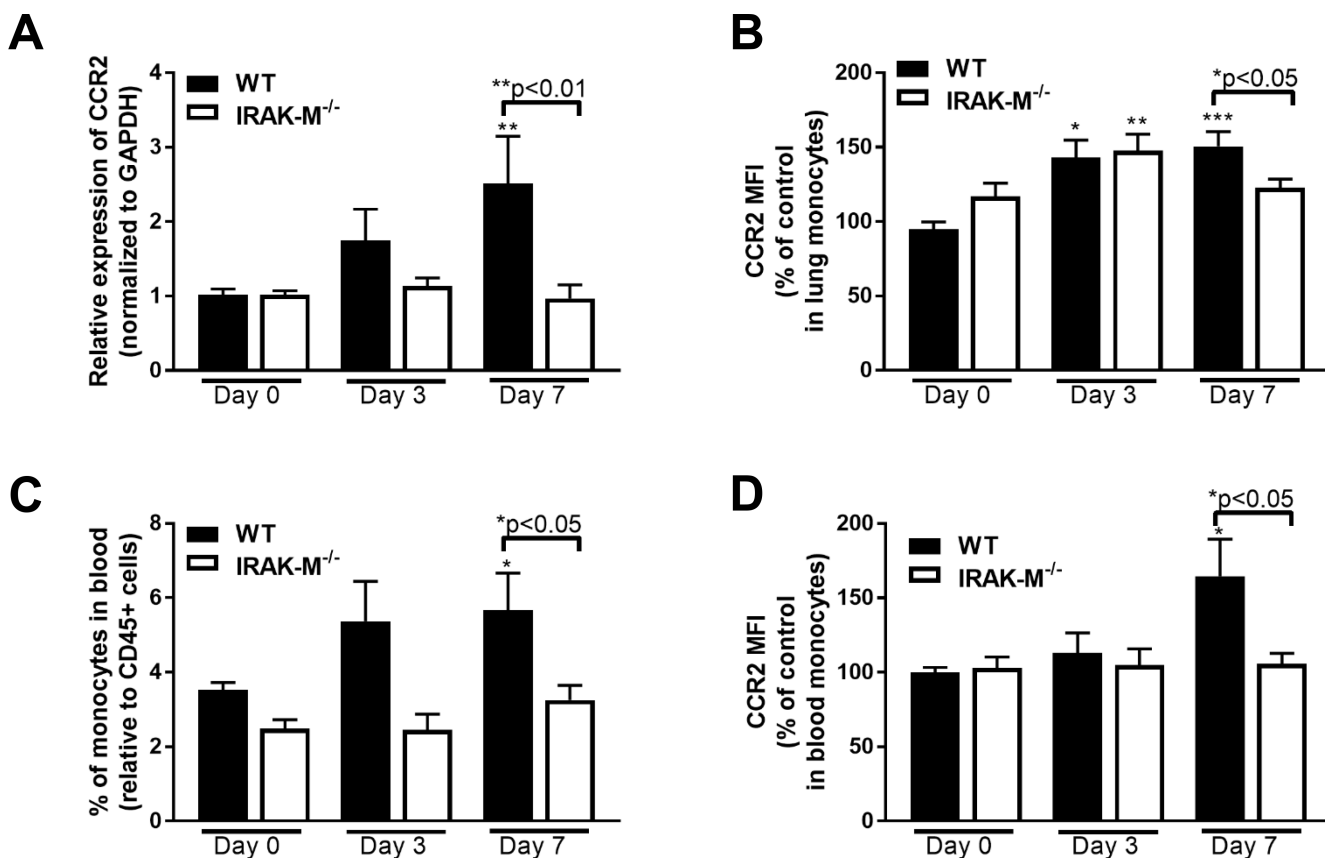


**Figure 3: Increased expression of CCR2 in IRAK-M<sup>-/-</sup> mice compared to WT controls following bleomycin challenge.**

WT and IRAK-M<sup>-/-</sup> mice were challenged with bleomycin (i.t). (A) Expression of CCR2 was by qPCR measured on adherence purified lung macrophages from WT and IRAK-M<sup>-/-</sup> mice following bleomycin challenge at the indicated timepoints. Data are representative of the analysis of n=5 samples/group that was repeated two times. (B) Expression of CCR2 was measured on monocytes isolated from the lungs of WT and IRAK-M<sup>-/-</sup> mice following bleomycin challenge via flow cytometry. Data are representative of the analysis of n=4 samples/group that was repeated three times. Blood was collected from WT and IRAK-M<sup>-/-</sup> mice and (C) the percentage of monocytes was measured in the blood and (D) the relative CCR2 expression on blood monocytes was determined by flow cytometry. Data are representative of the analysis of n=4 samples/group that was repeated two times. Statistical significance was determined by one-way ANOVA with Bonferroni correction. The asterisks (\*) represent statistical differences \*p<0.05, \*\*p<0.01, \*\*\*p<0.001.

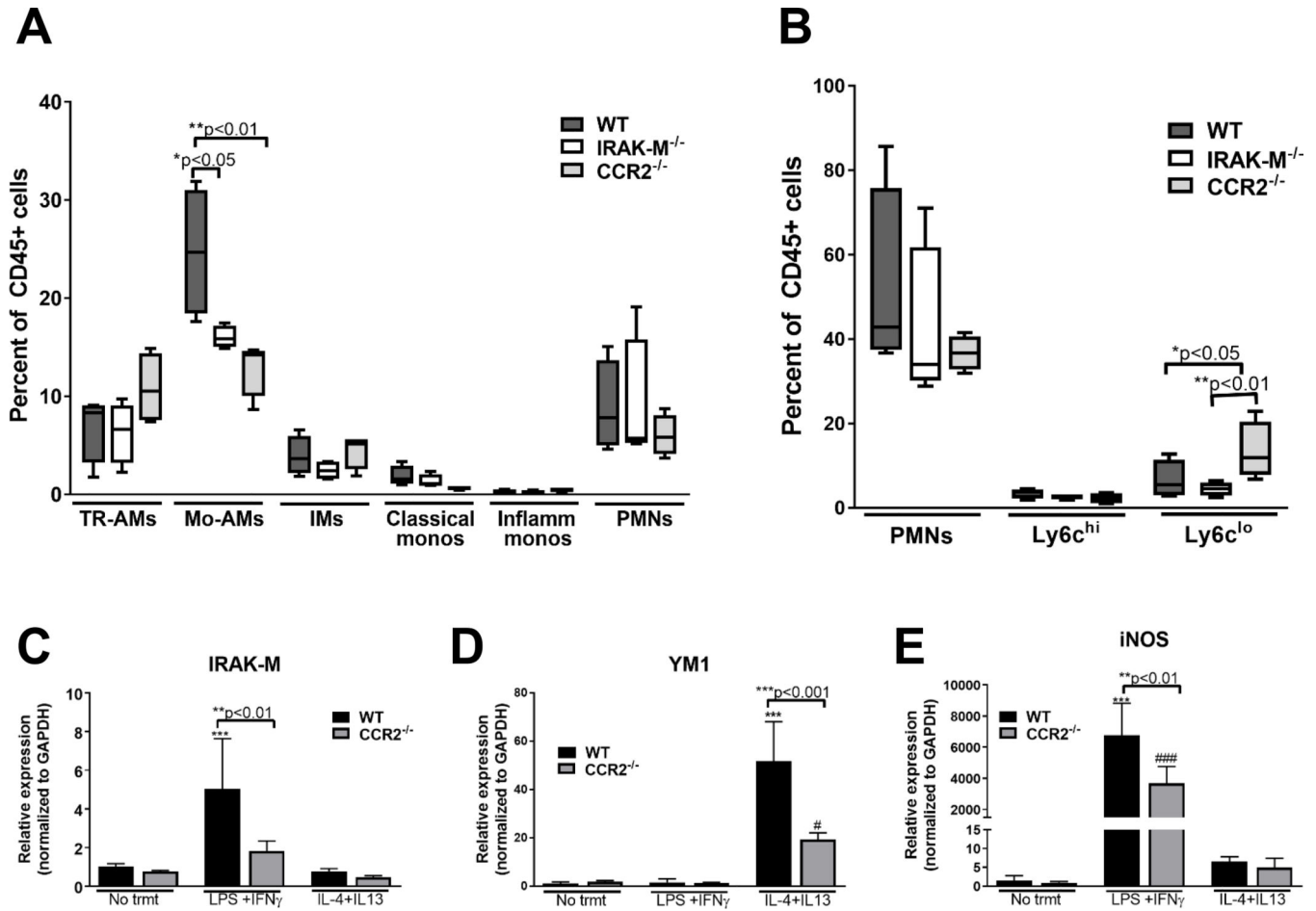


**Figure 4: CCR2 deficiency results in reduced monocyte recruitment to the lungs following bleomycin challenged *in vivo* and decreased IRAK-M expression and macrophage skewing responses *in vitro*.**

WT, IRAK-M<sup>-/-</sup> and CCR2<sup>-/-</sup> mice were challenged with bleomycin (i.t.) and whole tissue (A) and blood (B) was collected after 7 days, and the relative percent of CD45<sup>+</sup> cells was measured in each of these samples using the gating schemes previously outlined in Supplemental Figure 1 and 2. Data are representative of the analysis of n=4 samples/group. (C) BMDMs were grown from WT or CCR2<sup>-/-</sup> mice as described in the material and methods section and gene expression was measured via qPCR in unstimulated, classically activated (100 ng/ml of LPS and 20 ng/ml IFN $\gamma$ ), or alternatively activated (20 ng/ml of IL-4 and IL-13) conditions. Data represent the analysis of n=4 samples/group. Statistical significance was determined by one-way ANOVA with Bonferroni correction. The asterisks (\*) and pound sign (#) represent statistical differences: \*\*\*p<0.001 when compared to WT untreated and #p<0.05 and ###p<0.001 when compared to IRAK-M<sup>-/-</sup> untreated.

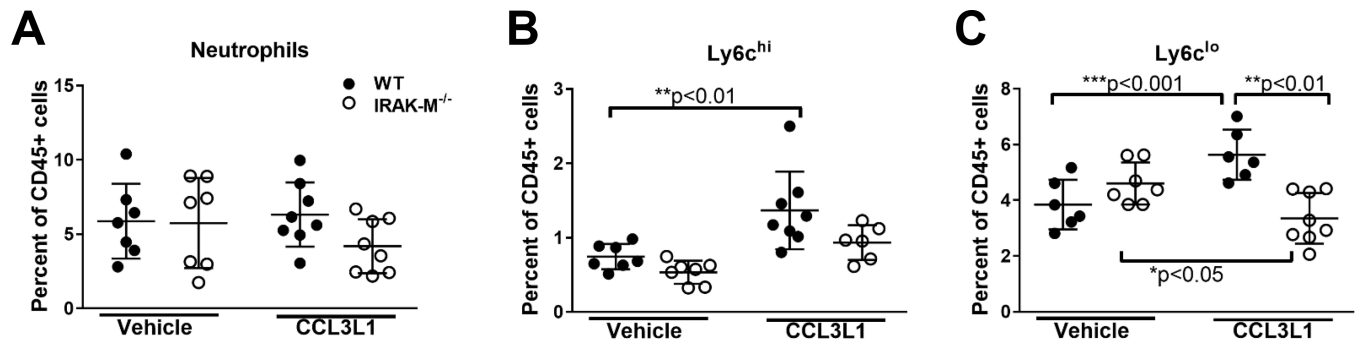


**Figure 5: Expression of IRAK-M alters monocytes mobilization from the bone marrow**  
 WT and IRAK-M<sup>-/-</sup> mice were treated with CCL3L1 or vehicle control (i.p.) and blood was collected 1 h later. The relative number of (A) neutrophils (CD45<sup>+</sup>Ly6g<sup>+</sup>), (B) classical monocytes (CD45<sup>+</sup>Ly6g<sup>-</sup>CD11b<sup>+</sup>Ly6c<sup>lo</sup>), and (C) inflammatory monocytes (CD45<sup>+</sup>Ly6g<sup>-</sup>CD11b<sup>+</sup>Ly6c<sup>hi</sup>) were determined by flow cytometry based on the gating strategy shown in Supplemental Figure 2A. Data represent the analysis of n =7/group. Statistical significance was determined by one-way ANOVA with Bonferroni correction. The asterisks (\*) represent statistical differences \*p<0.05, \*\*p<0.01, \*\*\*p<0.001.



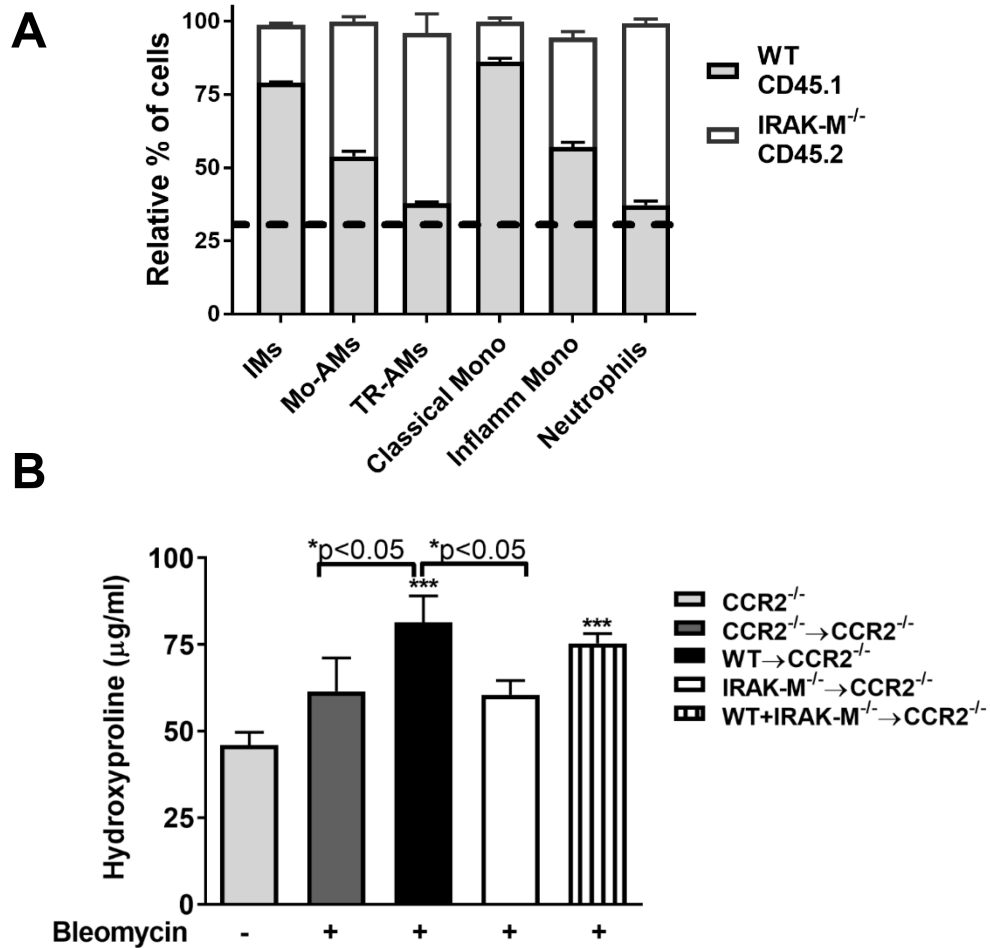


**Figure 6: IRAK-M expressing cells are recruited to the lung following bleomycin challenge in a competitive bone marrow transplant (BMT) model.**

Bone marrow (BM) chimeras were created by transplanting isolated BM from WT (CD45.1) mice and IRAK-M<sup>-/-</sup> (CD45.2) donor mice alone or in combination into lethally-irradiated CCR2<sup>-/-</sup> recipient mice. (A) The relative percentage of various monocyte, macrophage, and neutrophil populations in the lungs of the CD45.1/CD45.2 BM chimera mouse was measured using the gating scheme presented in Supplemental Figure 1. The dotted line represents the relative reconstitution rates of WT CD45.1 (light gray) compared to IRAK-M<sup>-/-</sup> CD45.2 (white) cells, as described in Supplemental Figure 6. (B) The amount of hydroxyproline was determined in the lung tissue of BM chimera mice compared to CCR2<sup>-/-</sup> mice who received no BMT. Data represent the analysis of n=4 samples/group. Statistical significance was determined by one-way ANOVA with Bonferroni correction. The asterisks (\*) represent statistical differences \*p<0.05, \*\*\*p<0.001.

**Table 1:**

List of antibodies used for flow cytometry experiments

Marker	Clone	Company
CD45	30-F11	Biolegend
CD64	X54-5/7.1	Biolegend
CD11b	M1/70	Biolegend
MHC II	M5/114.14.2	Biolegend
Ly6c	HK1.4	Biolegend
CCR2	475301	R&D Systems
CD11c	N418	Biolegend
Ly6g	1A8	Biolegend
Siglec F	E50-2240	BD Biosciences
CD45.1	A20	Biolegend
CD45.2	104	Biolegend

Author Manuscript

Author Manuscript

Author Manuscript

Author Manuscript

**Table 2:**

List of primers used for qPCR

Gene Name	Forward Primer	Reverse Primer
CCR2	ACACCCTGTTTCGCTGTAGG	GATTCCTGGAAGGTGGTCAA
ICAM1	TTCACACTGAATGCCAGCTC	GTCTGCTGAGACCCCTCTTG
ICAM2	ATCAACTGCAGCACCAACTG	ATCAACTGCAGCACCAACTG
VCAM1	CCCAGGTGGAGGTCTACTCA	CAGGATTTGGGAGCTGGTA
IRAK-M	CTGGCTGGATGTTTCGTCATATT	GGAGAACCTCTAAAAGGTCGC
YM1	CAGGTCTGGCAATCTTCTGAA	GTCTTGCTCATGTGTGTAAGTGA
iNOS	GTTCTCAGCCCAACAATAAAGA	GTGGACGGGTCGATGTCAC

Author Manuscript

Author Manuscript

Author Manuscript

Author Manuscript